

Provided for non-commercial research and education use.
Not for reproduction, distribution or commercial use.



This article appeared in a journal published by Elsevier. The attached copy is furnished to the author for internal non-commercial research and education use, including for instruction at the authors institution and sharing with colleagues.

Other uses, including reproduction and distribution, or selling or licensing copies, or posting to personal, institutional or third party websites are prohibited.

In most cases authors are permitted to post their version of the article (e.g. in Word or Tex form) to their personal website or institutional repository. Authors requiring further information regarding Elsevier's archiving and manuscript policies are encouraged to visit:

<http://www.elsevier.com/authorsrights>



Contents lists available at ScienceDirect

Journal of Quantitative Spectroscopy & Radiative Transfer

journal homepage: www.elsevier.com/locate/jqsrt

Time-dependent radiation characteristics of *Nannochloropsis oculata* during batch culture



Ri-Liang Heng, Laurent Pilon*

Mechanical and Aerospace Engineering Department, Henry Samueli School of Engineering and Applied Science, University of California, 420 Westwood Plaza, Eng. IV 37-132, Los Angeles, CA 90095, USA

ARTICLE INFO

Article history:

Received 31 October 2013

Received in revised form

10 April 2014

Accepted 12 April 2014

Available online 18 April 2014

Keywords:

Microalgae

Radiation characteristics

Nitrogen starvation

Photobioreactors

Biofuel

Photoacclimation

ABSTRACT

This paper reports the temporal evolution of the scattering and absorbing cross-sections of marine eustigmatophycease *Nannochloropsis oculata* grown in a flat-plate photobioreactor (PBR). The PBR was operated in batch mode under constant irradiance of 7500 or 10,000 lux provided by red LEDs emitting at 630 nm. The radiation characteristics between 400 and 750 nm and pigment concentrations of *N. oculata* were measured systematically every 24 h for up to 18 days. They were found to vary significantly with time in response to changes in light and nutrients availability. The results were interpreted in terms of up- and down-regulations of pigments and other intracellular components. Finally, this study demonstrates that the light transfer in the PBR could be predicted using constant radiation characteristics measured during the exponential growth phase with reasonable accuracy provided that the cultures were not nitrogen limited. During nitrogen starvation, pigment concentrations decreased and radiation characteristics evolved rapidly. These results will be useful in the design and operation of PBRs for biofuel production at both small and large scales.

© 2014 Elsevier Ltd. All rights reserved.

1. Introduction

Cultivation of microalgae offers green, sustainable, and potentially low-cost solutions in a variety of applications. For example, microalgae could be used to remove metal contaminants, phosphates, and nitrates from effluent water [1]. This method is less energy-intensive than traditional wastewater treatment methods. Also, microalgae are able to produce a variety of useful products namely (i) lipids which can be converted into biodiesel [2], (ii) hydrogen [3], (iii) fertilizers [1,4], and (iv) nutritional supplements [1]. Despite promising potentials, significant scientific and technological advancements are required before widespread commercialization can be achieved.

Microalgae are typically suspended in growth medium and cultivated in open pond systems or closed photobioreactors (PBRs) [2]. Batch operation is often preferred over continuous operation for industrial scale PBRs for their simplicity, flexibility, and low cost [5]. To maximize biomass productivity, microalgae strains are usually selected for their rapid growth rate and their ability to tolerate high biomass concentration [6]. To achieve large PBR productivity, photosynthetic microorganisms require an optimal irradiance. At high biomass concentrations, light penetration in the PBR can become severely limiting [7]. Then, a large fraction of the PBR volume may receive insufficient energy to carry out photosynthesis leading to a significant decrease in biomass productivity. Similarly, excessive irradiance results in photoinhibition which also severely hampers growth rates [8]. To counteract these non-optimal light conditions, photosynthetic microorganisms are able to photoacclimate by either increasing or decreasing the

* Corresponding author. Tel.: +1 310 206 5598; fax: +1 310 206 2302.
E-mail address: pilon@seas.ucla.edu (L. Pilon).

number and size of their photosynthetic units [9]. This enables control over the energy input driving photosynthesis in the cells. Moreover, upon exposure to large irradiance, the decrease in cellular chlorophyll concentration is facilitated by dilution due to cell division [10]. By contrast, under small irradiance, the cells should increase their chlorophyll concentrations at a fast enough rate to compensate for dilution due to cell division. Therefore, microorganisms adapt faster to large irradiance than to small irradiance [10]. Overall, proper light distribution in the PBR is essential for the economic viability of large scale microalgae cultivation systems.

Most cell photosynthetic pigments absorb light in the so-called photosynthetically active radiation (PAR) region from 400 to 700 nm [11]. In addition, the refractive index mismatch between cells and the growth medium causes incident light to be scattered [12]. The absorption and scattering properties of microalgae are species-specific and can be obtained either through experimental measurements [13–15] or from model predictions based on electromagnetic wave theory [16–20]. These properties are usually assumed to be time-invariant despite changes in size and composition as the microalgae adapt to changing growth conditions [7,13–15,17–19,21–24]. Moreover, in order to enhance lipid accumulation, microalgae are deprived of nitrogen through sudden or progressive starvation [25]. As a result, the microalgae culture changes color from green to yellow/brown.

Overall, it is important to consider the impact of photoacclimation and nutrient limitation or starvation (particularly nitrogen) on light transfer in PBRs. Changes in growth conditions are typically encountered during the course of batch operation. The goal of this study is to measure the temporal evolution of the radiation characteristics of microalgae during batch growth and to provide physiological interpretation. The results will be used to assess the impact on light transfer in PBRs. The marine eustigmatophycease *Nannochloropsis oculata* was chosen as a model organism for its high lipid content and high biomass productivity [2,25].

1.1. Light transfer

Light transfer in a homogeneous absorbing, scattering, and non-emitting microalgal suspension is governed by the radiative transfer equation (RTE) written as [7]

$$\hat{\mathbf{s}} \cdot \nabla I_\lambda(\mathbf{r}, \hat{\mathbf{s}}) = -\kappa_\lambda I_\lambda(\mathbf{r}, \hat{\mathbf{s}}) - \sigma_{s,\lambda} I_\lambda(\mathbf{r}, \hat{\mathbf{s}}) + \frac{\sigma_{s,\lambda}}{4\pi} \int_{4\pi} I_\lambda(\mathbf{r}, \hat{\mathbf{s}}_i) \Phi_{T,\lambda}(\hat{\mathbf{s}}_i, \hat{\mathbf{s}}) d\Omega_i \quad (1)$$

where I_λ is the spectral radiation intensity about the direction $\hat{\mathbf{s}}$ at location \mathbf{r} (in $\text{W}/\text{m}^2 \text{sr nm}$) while κ_λ and $\sigma_{s,\lambda}$ are the effective spectral absorption and scattering coefficients of the suspension (in m^{-1}), respectively. The first and second terms on the right-hand side of Eq. (1) correspond to attenuation of the intensity $I_\lambda(\mathbf{r}, \hat{\mathbf{s}})$ along direction $\hat{\mathbf{s}}$ caused by absorption and scattering, respectively. The third term accounts for multiple scattering, i.e., for the fact that a fraction of intensity $I_\lambda(\mathbf{r}, \hat{\mathbf{s}}_i)$ from direction $\hat{\mathbf{s}}_i$ may be scattered in direction $\hat{\mathbf{s}}$. The scattering phase function $\Phi_{T,\lambda}(\hat{\mathbf{s}}_i, \hat{\mathbf{s}})$ represents the probability that

radiation propagating in the solid angle $d\Omega_i$ around direction $\hat{\mathbf{s}}_i$ be scattered into the solid angle $d\Omega$ along direction $\hat{\mathbf{s}}$. It is normalized such that

$$\frac{1}{4\pi} \int_{4\pi} \Phi_{T,\lambda}(\hat{\mathbf{s}}_i, \hat{\mathbf{s}}) d\Omega_i = 1 \quad (2)$$

The absorption and scattering coefficients are related, respectively, to the average absorption $\bar{C}_{abs,\lambda}$ and scattering $\bar{C}_{sca,\lambda}$ cross-sections (in m^2) by the microalgae cell number density N_T , defined as the number of cells per m^3 of suspension, according to [7]

$$\kappa_\lambda = \bar{C}_{abs,\lambda} N_T \quad \text{and} \quad \sigma_{s,\lambda} = \bar{C}_{sca,\lambda} N_T \quad (3)$$

The extinction coefficient is defined as $\beta_\lambda = \kappa_\lambda + \sigma_{s,\lambda}$.

Pottier et al. [18] derived an analytical solution to the RTE using the generalized two-flux approximation considering one-dimensional light transfer through a well-mixed algal suspension in a vertical flat-plate PBR of thickness L . The front window ($z=0$) was assumed to be transparent and exposed to irradiance $G_{in,\lambda}$ incident at an angle θ_c with respect to the direction normal to the PBR window. The back surface ($z=L$) was diffusely reflecting with reflectance ρ_λ . The local spectral fluence rate $G_\lambda(z)$ in the PBR, corresponding to the total intensity impinging at location z from all directions, i.e., $G_\lambda(\mathbf{r}) = \int_{4\pi} I_\lambda(\hat{\mathbf{s}}, \mathbf{r}) d\Omega$, was expressed as [18]

$$\frac{G_\lambda(z)}{G_{in,\lambda}} = 2 \sec \theta_c \times \frac{[\rho_\lambda(1+\alpha_\lambda)e^{-\delta_\lambda L} - (1-\alpha_\lambda)e^{-\delta_\lambda L}]e^{\delta_\lambda z} + [(1+\alpha_\lambda)e^{\delta_\lambda L} - \rho_\lambda(1-\alpha_\lambda)e^{\delta_\lambda L}]e^{-\delta_\lambda z}}{(1+\alpha_\lambda)^2 e^{\delta_\lambda L} - (1-\alpha_\lambda)^2 e^{-\delta_\lambda L} - \rho_\lambda(1-\alpha_\lambda^2)e^{\delta_\lambda L} + \rho_\lambda(1-\alpha_\lambda^2)e^{-\delta_\lambda L}} \quad (4)$$

where α_λ and δ_λ are expressed as [18]

$$\alpha_\lambda = \sqrt{\frac{\bar{C}_{abs,\lambda}}{\bar{C}_{abs,\lambda} + 2b_\lambda \bar{C}_{sca,\lambda}}}, \quad \delta_\lambda = N_T \sec \theta_c \sqrt{\bar{C}_{abs,\lambda}(\bar{C}_{abs,\lambda} + 2b_\lambda \bar{C}_{sca,\lambda})} \quad (5)$$

The backward scattering ratio b_λ for an axisymmetric phase function is defined as [18]

$$b_\lambda = \frac{1}{2} \int_{\pi/2}^{\pi} \Phi_{T,\lambda}(\theta) \sin \theta d\theta \quad (6)$$

where θ is the scattering angle between directions $\hat{\mathbf{s}}_i$ and $\hat{\mathbf{s}}$.

The average fluence rate G_{ave} can be defined as the volume- and PAR-averaged local fluence rate $G_\lambda(z)$ per unit surface area of PBR expressed as [7]

$$G_{ave} = \frac{1}{L} \int_{400}^{700} \int_0^L G_\lambda(z) dz d\lambda \quad (7)$$

The average radiant power absorbed per cell present in the PBR over the PAR region denoted by A_{ave} (in $\mu\text{mol}/\text{s}/\text{cell}$) was defined as [22]

$$A_{ave} = \frac{1}{L} \int_0^L \int_{400}^{700} \bar{C}_{abs,\lambda} G_\lambda(z) d\lambda dz \quad (8)$$

This quantity (or $A_{ave} N_T$) enables the formulation of models coupling radiant light transfer and microalgae metabolism and growth kinetics in PBRs [22].

1.2. *Nannochloropsis oculata*

N. oculata microalgae consist of spheroidal cells approximately 2–3 μm in diameter. They possess the pigments Chlorophyll (Chl) *a* and carotenoids. Chl *a* is a crucial pigment in the photosynthetic process [1]. It absorbs mainly blue and red photons and transfers charges by resonance energy transfer to the reaction centers. On the other hand, carotenoids serve as accessory pigments that can be either photosynthetic (PSC) or photoprotective (PPC). Photosynthetic carotenoids absorb green and yellow light and thus broaden the microalgae absorption spectrum [26]. Photoprotective carotenoids prevent photo-damage to a light harvesting apparatus by converting excess light energy into heat [26]. More specifically, the *in vivo* absorption peaks of Chl *a* are centered around 435, 630, and 676 nm while carotenoids absorb most strongly between 400 and 550 nm [11].

The present study reports the temporal evolution of the absorption and scattering cross-sections of *N. oculata* during batch growth. The impact of physiological adaptations on the microalgae absorption and scattering cross-sections during the different phases of their growth was investigated. The results were used to assess the evolution of light transfer in flat plate PBRs operated in batch mode and to evaluate the validity of the commonly made assumption that microalgae radiation characteristics remain constant during their growth.

2. Materials and methods

2.1. Cultivation and sample preparation

The microalgae species *N. oculata* UTEX LB 2164 was purchased from UTEX Austin, TX. It was cultivated in artificial sea water medium in 250 ml culture bottles fitted with vented caps and exposed to a continuous luminous flux of 2800–3000 lux provided by fluorescent light bulbs (GroLux by Sylvania, USA). The artificial seawater medium had the following composition (per liter of distilled water): NaCl 18 g, $\text{MgSO}_4 \cdot 7\text{H}_2\text{O}$ 2.6 g, KCl 0.6 g, NaNO_3 1 g, $\text{CaCl}_2 \cdot 2\text{H}_2\text{O}$ 0.3 g, KH_2PO_4 0.05 g, NH_4Cl 0.027 g, $\text{Na}_2\text{EDTA} \cdot 2\text{H}_2\text{O}$ 0.03 g, H_3BO_3 0.0114 g, $\text{FeCl}_3 \cdot 6\text{H}_2\text{O}$ 2.11 mg, $\text{MnSO}_4 \cdot \text{H}_2\text{O}$ 1.64 mg, $\text{ZnSO}_4 \cdot 7\text{H}_2\text{O}$ 0.22 mg, $\text{CoCl}_2 \cdot 6\text{H}_2\text{O}$ 0.048 mg, and vitamin B_{12} 0.135 mg.

After 11 days of growth under continuous fluorescent light, 10 ml of the culture was transferred into a 2 cm thick PMMA flat plate PBR. The culture was then diluted with 240 ml of growth medium and the batch experiment started. The PBR was exposed to an illuminance of 7500 or 10,000 lux (222 or 296 $\mu\text{mol photon/m}^2 \text{ s}$) from red LEDs (C503B-RAN Cree, USA) with peak wavelength at 630 nm and a spectral bandwidth of 30 nm. The culture was continuously sparged with 50 cm^3/min of air with 2 vol % of CO_2 passed through a glass fiber filter of pore size 0.3 μm (HEPA-Vent by Whatman, USA). The entire setup was placed on an orbital shaker operated at 90 rpm to ensure well-mixed conditions and to keep the microorganisms in suspension. The temperature was kept constant at 23 °C.

In order to obtain accurate radiation characteristic measurements, the samples taken in the early stages of the batch growth (day 0–2) had to be concentrated to achieve higher optical signal-to-noise ratio. Note that the small cell concentration rendered centrifugation of the sample impossible. In addition, absorption and scattering by the growth medium at these low concentrations were not negligible compared with those of *N. oculata*. Thus, prior to optical measurements, 10 ml of the culture suspension was filtered using 0.45 μm pore size cellulose membrane filters (HAWP-04700 by Millipore, USA). The cells were washed off the filter with 3 ml of phosphate buffer saline (PBS) solution and collected. The growth medium was replaced with non-absorbing PBS solution to achieve the desired microalgae concentration. Upon reaching a sufficiently dense culture, absorption by the growth medium was negligible compared with that of the microalgae and there was no need to concentrate the samples. In fact, samples with high cell concentrations (after day 6) were diluted with PBS to avoid multiple scattering during transmission measurements.

Finally, cell number density N_T of the culture (in $\#/ \text{m}^3$) and the distribution of cell diameter $f(d_s)$ based on the equivalent projected area were measured every 24 h using an automatic cell counter (Nexcelom Cellometer Auto M10). To do so, 20 μl of a well mixed culture was pipetted into a disposable hemocytometer (Nexcelom CHT4-SD100). The device counted the number of cells present in the known volume of the hemocytometer through the use of 2D micrographs. Each cell density measurement reported corresponded to the average cell count of two samples, each counted twice.

2.2. Radiation characteristics

The average absorption and scattering cross-sections of *N. oculata* were measured every 24 h for up to 18 days. The following assumptions were made during data analysis: (1) the microalgae suspension was well mixed and randomly oriented, (2) single scattering prevailed thanks to the low cell densities considered, and (3) the scattering phase function was assumed to be time-invariant and constant over the PAR region. Kandilian et al. [27] measured, with a polar nephelometer, the scattering phase function at 633 nm for *N. oculata* grown under red LEDs in artificial sea water medium. The backward scattering ratio b_λ was reported to be 0.0019. They also retrieved the complex index of refraction and verified that the scattering phase function was nearly independent of wavelength over the PAR region. The growth conditions and measured diameters of *N. oculata* cells reported in their study were similar to that in the present study. Therefore, these prior measurements were adopted.

The extinction coefficient of the microalgae suspension β_λ was obtained from normal–normal transmittance measurements, denoted by $T_{n,\lambda}$, after correcting for forward scattering by the suspension [28]. The measurements were performed in 1 cm pathlength cuvettes using a UV–VIS spectrophotometer (Shimadzu, USA, Model UV-3103PC) from 400 to 750 nm with 1 nm spectral resolution as illustrated in Fig. 1a. In order to correct for the effects of

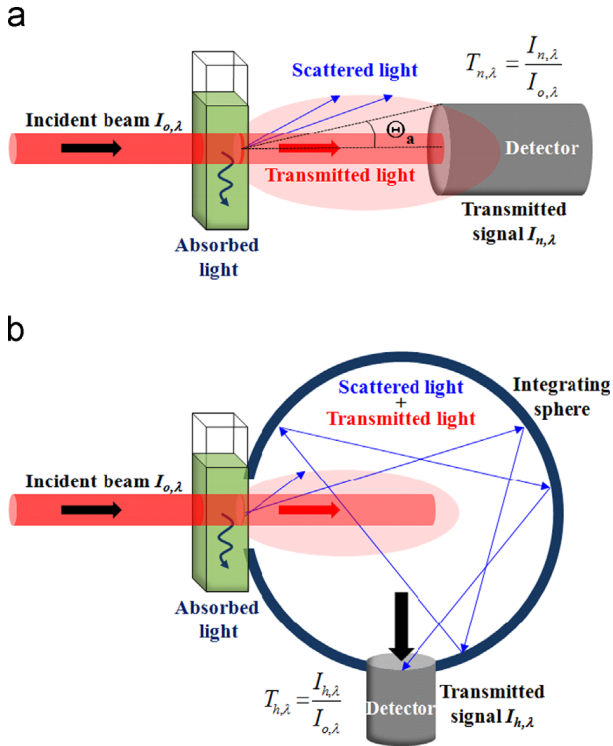


Fig. 1. Schematic of experimental setup used to determine (a) the extinction coefficient β_λ from normal-normal spectral transmittance and (b) the absorption coefficient κ_λ from normal-hemispherical spectral transmittance.

reflection and refraction by the cuvette, the measurements were calibrated using the transmittance of the reference medium (e.g., PBS) denoted by $T_{n,\lambda,ref}$. Then, the apparent extinction coefficient χ_λ was defined as [28,29]

$$\chi_\lambda = -\frac{1}{t} \ln\left(\frac{T_{n,\lambda}}{T_{n,\lambda,ref}}\right) \quad (9)$$

The detector had a finite size and detected a portion of the light scattered in the forward direction. This effect needed to be corrected for since *N. oculata* cells are largely forward scattering [27]. The apparent extinction coefficient was related to the actual absorption and scattering coefficients by [28,29],

$$\chi_\lambda = \kappa_\lambda + \sigma_{s,\lambda} - \epsilon_n \sigma_{s,\lambda} \quad (10)$$

where ϵ_n represents the fraction of scattered light reaching the detector and was expressed as [30,31]

$$\epsilon_n = \frac{1}{2} \int_0^{\theta_a} \Phi_{T,\lambda}(\theta) \sin \theta \, d\theta \quad (11)$$

where θ_a is the half acceptance angle of the detector while the scattering phase function $\Phi_{T,\lambda}$ of *N. oculata* was measured by Kandilian et al. [27].

The absorption coefficient κ_λ was obtained from normal-hemispherical transmittance measurements, denoted by $T_{h,\lambda}$, performed with an integrating sphere (ISR-3100 by Shimadzu, USA) at wavelengths from 400 to 750 nm as illustrated in Fig. 1b [13]. Then, the apparent absorption

coefficient $\chi_{h,\lambda}$ can be expressed as

$$\chi_{h,\lambda} = -\frac{1}{t} \ln\left(\frac{T_{h,\lambda}}{T_{h,\lambda,ref}}\right) \quad (12)$$

Due to imperfect reflections at the inner surface of the integrating sphere and the geometry of the experimental setup, the detector was unable to capture all the scattered light. In order to correct for these errors, the apparent absorption coefficient can be related to the absorption and scattering coefficients by

$$\chi_{h,\lambda} = \kappa_\lambda + (1 - \epsilon_h) \sigma_{s,\lambda} \quad (13)$$

where ϵ_h represents the fraction of scattered light detected by the integrating sphere and was assumed to be constant over the PAR region. Davis-Colley et al. [29] assumed that the microalgae did not absorb radiation at wavelength λ_o (e.g. $\lambda_o = 750$ nm for *N. oculata* [27]). At this wavelength, the absorption coefficient $\kappa_\lambda = 0$ and ϵ_h can be retrieved from Eq. (13) according to

$$\epsilon_h = 1 - \frac{\chi_{h,\lambda_o}}{\sigma_{s,\lambda_o}} \quad (14)$$

Similarly, the apparent extinction coefficient at wavelength λ_o can be retrieved from Eq. (10) as

$$\chi_{\lambda_o} = (1 - \epsilon_n) \sigma_{s,\lambda_o} \quad (15)$$

Combining Eqs. (10), (13), (14), and (15), the actual absorption coefficient κ_λ can be obtained using the following expression:

$$\kappa_\lambda = \chi_{h,\lambda} - \chi_{h,\lambda_o} \frac{\sigma_{s,\lambda}}{\sigma_{s,\lambda_o}} \quad \text{where} \quad \frac{\sigma_{s,\lambda}}{\sigma_{s,\lambda_o}} = \frac{\chi_\lambda - \chi_{h,\lambda}}{\chi_{\lambda_o} - \chi_{h,\lambda_o}} \quad (16)$$

Finally, the actual extinction coefficient β_λ can be obtained by substituting κ_λ into Eq. (10). Then, the scattering coefficient was computed using the definition $\sigma_{s,\lambda} = \beta_\lambda - \kappa_\lambda$.

Note that the samples were manually shaken prior to the transmission measurements so as to minimize the effects of sedimentation. Each measurement was performed with two samples of different cell densities. The sample normal-normal and normal-hemispherical transmittances were measured three times and the results were averaged. The absorption and scattering coefficients κ_λ and $\sigma_{s,\lambda}$ were divided by the samples' respective cell number density N_T to obtain the average absorption and scattering cross-sections $\bar{C}_{abs,\lambda}$ and $\bar{C}_{sca,\lambda}$ according to Eq. (3). Van de Hulst [32] suggested that "a simple and conclusive test for the absence of multiple scattering" consists of demonstrating that scattering intensity is directly proportional to the particle concentration. In other words, the spectral cross-sections $\bar{C}_{abs,\lambda}$ and $\bar{C}_{sca,\lambda}$ for different cell densities should collapse onto a single line if single and independent scattering prevailed. This provided further validation of the experimental procedure and data analysis.

2.3. Chemical analysis

The pH of each sample was determined with a pH meter (Omega PHB-212). This provided an indirect method for monitoring CO_2 concentrations in the culture. Indeed, dissociation of CO_2 in water causes the solution to become slightly acidic. Therefore, an increase in pH could be

interpreted as lower CO₂ concentration in the microalgae culture.

Pigment concentrations were determined spectrophotometrically using the method reported by Wellburn [33]. A 2 ml sample of microalgae culture was centrifuged for 2 min at 10,000 rpm (6500g) and the supernatant discarded. Then, 3 ml of methanol was added to the cell pellet. The sample was vortexed for 1 min followed by sonication for 4 min. This ensured that the microalgae cell walls were broken down. The sample was left in a dark room for 24 h before being centrifuged to remove cell debris. The supernatant was extracted and transferred into 1 cm pathlength polystyrene cuvettes for normal-normal transmittance ($T_{n,\lambda}$) measurements at 480, 666, and 750 nm. The corresponding optical density (OD) was defined as $OD_\lambda = -\ln T_{n,\lambda}$. Pigment extraction was performed in duplicates and OD measurements in triplicates. Chl *a* concentration C_{chla} (in $\mu\text{g}/\text{m}^3$ of suspension) was determined from the OD measurements according to [33]

$$C_{chla} = 15.65(OD_{666} - OD_{750})v/Vl \quad (17)$$

where V is the microalgae sample volume (in m^3), v is the volume of methanol (in m^3), and l is the pathlength of the cuvette (in cm), taken as $V=2$ ml, $v=3$ ml, and $l=1$ cm. Similarly, the total carotenoid concentration C_{x+c} including both PSC and PPC was calculated as [34]

$$C_{x+c} = 4(OD_{480} - OD_{750})v/Vl \quad (18)$$

The pigment concentration (in $\mu\text{g}/\text{cell}$) was estimated as the ratio of the mass of pigment mass per unit volume (in $\mu\text{g}/\text{m}^3$) to the cell number density N_T (in $\#/\text{m}^3$). For the culture grown under 10,000 lux, pigment extractions were only conducted after 145 h in order to preserve culture volume and to investigate the behavior of the pigment concentrations in the later stages of microalgae growth during nitrogen starvation.

3. Results and discussions

3.1. Cell growth

Fig. 2 shows the temporal evolution of the cell number density N_T for microalgae cultures grown under 7500 and 10,000 lux. Each data point represents the arithmetic mean of the measurements and the error bars correspond to one standard deviation. The growth curves exhibited the typical microalgal growth phases namely (i) the lag phase, (ii) the exponential phase, and (iii) the stationary phase. For both incident irradiances, the lag phase was characterized by slow initial growth rates and occurred approximately between 0 and 50–75 h. It can be attributed to the microalgae's adaptation to drastically different growth conditions after their transfer from the culture bottle to the PBR [35]. The exponential phase occurred immediately after the lag phase and was characterized by large growth rates. *N. oculata* cultures grew faster under 10,000 lux than under 7500 lux. The stationary phase occurred after approximately 225 and 275 h for cultures grown under 10,000 and 7500 lux, respectively. It could be due to insufficient light, nutrients, and/or CO₂. The cultures grown under 7500 and 10,000 lux reached about the

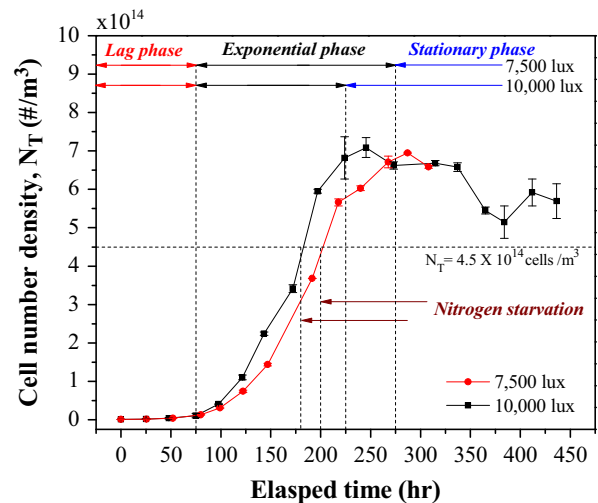


Fig. 2. Cell number density evolution with respect to growth times for *N. oculata* batch cultures grown under 7500 and 10,000 lux of red light. Lag, exponential, and stationary phases and onset of nitrogen starvation are also shown.

same maximum cell density of 6.8×10^{14} cells/ m^3 . It is important to note that the large fluctuations in number density N_T during the stationary phase were due to the formation of microalgae colonies that adhered to the inner surfaces of the PBR. However, subsequent measurements of the radiation characteristics remain correct because these colonies were not collected during sampling. Note also that the equivalent cell diameter d_s was 2.63 ± 0.5 μm and did not vary significantly with time.

Moreover, the pH of the culture remained between 7.6 and 8.2 and did not increase significantly during the microalgae growth. Chiu et al. [36] reported that *N. oculata* culture grown in continuous mode maintained a pH of 7.8 when aerated with air enriched with 2 vol % of CO₂. Despite the differences between batch and continuous modes, the pH was nearly similar. The slight increase in pH was caused by the growth of the microalgae and the corresponding increase in CO₂ uptake. These observations suggest that light and CO₂ availability were not limiting factors [36,37]. Thus, nutrient starvation was responsible for the stationary phase.

Elemental analysis similar to that reported by Kandilian et al. [27] for the same microalgae species grown in the Erdshribers medium was performed in the present study for artificial sea water medium. It predicted that the culture experienced nitrogen starvation at dry biomass concentrations of 1.72 g/L. This dry biomass concentration can be converted into cell number densities by treating *N. oculata* cells as spheres with an average diameter of 2.63 μm , water volume fraction taken as 0.7 [38], and dry biomass density taken as 1350 kg/m^3 [19]. Then, nitrogen starvation was expected to occur at $N_T = 4.5 \times 10^{14}$ cells/ m^3 . The cultures grown under 7500 and 10,000 lux reached this concentration after 200 and 180 h, respectively. These values show that the microalgae were actually nutrient limited midway through their exponential phase but continued growing to more than twice their concentrations before reaching the stationary phase.

3.2. Mass absorption and scattering cross-sections

Fig. 3a and b presents the average absorption cross-sections $\bar{C}_{abs,\lambda}$ of *N. oculata* grown under 7500 and 10,000 lux, respectively, in the spectral range from 400 to 750 nm at different times during their growth. The average absorption cross-section $\bar{C}_{abs,\lambda}$ displayed peaks at 435, 630, and 676 nm corresponding to in vivo absorption peaks of Chl *a* and at 485 nm corresponding to that of carotenoids. Similarly, Fig. 3c and d presents the average scattering cross-sections $\bar{C}_{sca,\lambda}$ of *N. oculata* grown under 7500 and 10,000 lux, respectively. The cross-sections $\bar{C}_{sca,\lambda}$ and $\bar{C}_{abs,\lambda}$ measured at time 0 h were similar for the two incident irradiances considered. This confirms that the initial conditions and experimental measurements were consistent. The absorption cross-section $\bar{C}_{abs,\lambda}$ features similar values and trends for both incident irradiances. For a given incident irradiance, $\bar{C}_{abs,\lambda}$ at wavelength λ in the PAR region varied significantly during the course of the experiments. For example, the relative difference between the minimum and maximum values of $\bar{C}_{abs,676}$ reached up to 226% for culture grown under 10,000 lux. The same

relative difference for $\bar{C}_{abs,485}$ reaches up to 145% for culture grown under 7500 lux.

Furthermore, for any given time and wavelength, the scattering cross-section $\bar{C}_{sca,\lambda}$ for *N. oculata* grown under 10,000 lux was systematically larger than those grown under 7500 lux while trends in their temporal evolution were similar. The scattering cross-section of a cell depends on its size and on the refractive index mismatch between the cell and the surrounding medium. The effective refractive index of the microalgae depends on their water content and their chemical composition [12,38]. The major cell constituents, namely proteins, carbohydrates, and lipids, do not absorb in the PAR region and have refractive indices larger than that of water. In addition, carbohydrates and proteins have larger refractive indices than lipids [38]. Carbohydrates and proteins concentrations in *N. oculata* were reported to increase at the expense of lipids when grown under larger incident irradiance [39]. This may explain why $\bar{C}_{sca,\lambda}$ was larger for microalgae grown under 10,000 lux than that under 7500 lux. Note also that carbohydrates, proteins, and lipids have an index of refraction nearly constant over the PAR region [38]

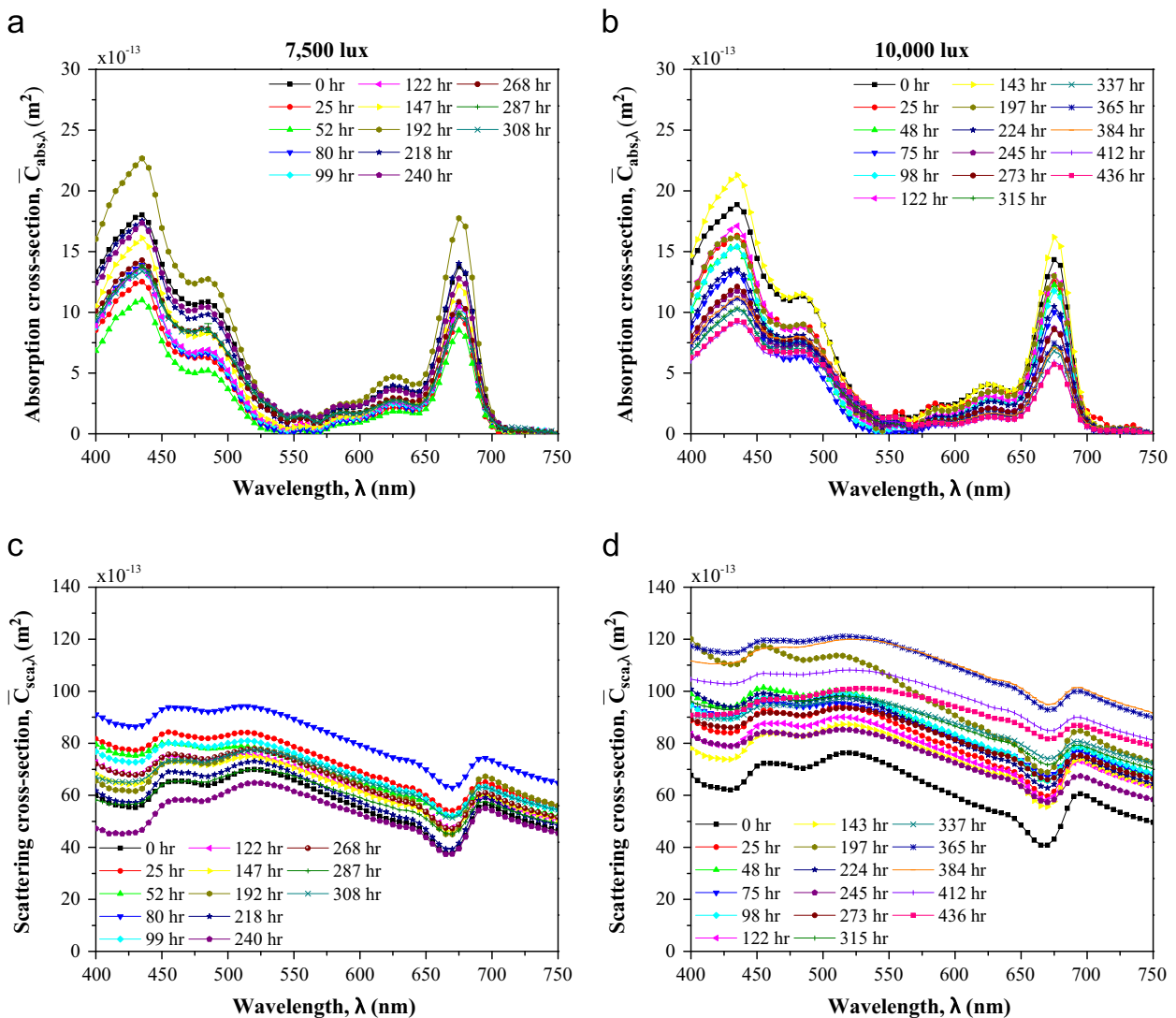


Fig. 3. (a) and (b) Average absorption cross-section $\bar{C}_{abs,\lambda}$ and (c) and (d) average scattering cross-section $\bar{C}_{sca,\lambda}$ in the spectral range from 400 to 750 nm for *N. oculata* grown under 7500 and 10,000 lux, respectively.

while the cell size distribution remains nearly unchanged over time. This could be the reason why $\bar{C}_{sca,\lambda}$ increased or decreased almost uniformly across the PAR over time.

It is also worth noting that dips in the scattering cross-sections $\bar{C}_{sca,\lambda}$ were observed around wavelengths corresponding to the absorption peaks in $\bar{C}_{abs,\lambda}$. This “cross-talk” between absorption and scattering cross-sections can be attributed to resonance behavior in the real part (or refraction index) of the complex index of refraction of the microalgae at wavelengths when the imaginary part (or absorption index) features strong absorption peaks. Such resonance is predicted by the Ketteler–Helmholtz theory [12], among others.

To illustrate the temporal evolution of the absorption cross-section, Fig. 4a and b plot $\bar{C}_{abs,\lambda}$ at wavelengths 485 nm and 676 nm with respect to time, respectively. These wavelengths correspond to carotenoids and Chl *a* absorption peaks, respectively. Similarly, Fig. 4c and d shows the measured Chl *a* and total carotenoids (PSC+PPC) concentrations as functions of time. Each data point represents the arithmetic mean of multiple

measurements and the error bars correspond to one standard deviation. It is evident that the trends in the absorption peaks $\bar{C}_{abs,676}$ and $\bar{C}_{abs,485}$ closely follow the trends in Chl *a* and PSC+PPC concentrations, respectively. In fact, $\bar{C}_{abs,676}$ and $\bar{C}_{abs,485}$ and the corresponding pigment concentration reach their maximum and minimum at the same times. The initial down-regulation of pigment was caused by exposure to excessive fluence rates when the suspensions featured relatively small cell number densities. It contributed to reducing the energy absorbed per cell to prevent photodamage to their light-harvesting antenna. It is interesting to note that the time frame during which pigment concentrations decreased closely coincided with the lag phase observed in the growth curves between 0 and 50–75 h (Fig. 2).

Moreover, Fig. 4c and d indicate that Chl *a* and carotenoids concentrations increased between times 50 and 200 h for the culture grown under 7500 lux and between 75 and 180 h for those grown under 10,000 lux. This was due to up-regulation of pigments by microalgae to avoid photolimitation. Indeed, due to rapid cell division

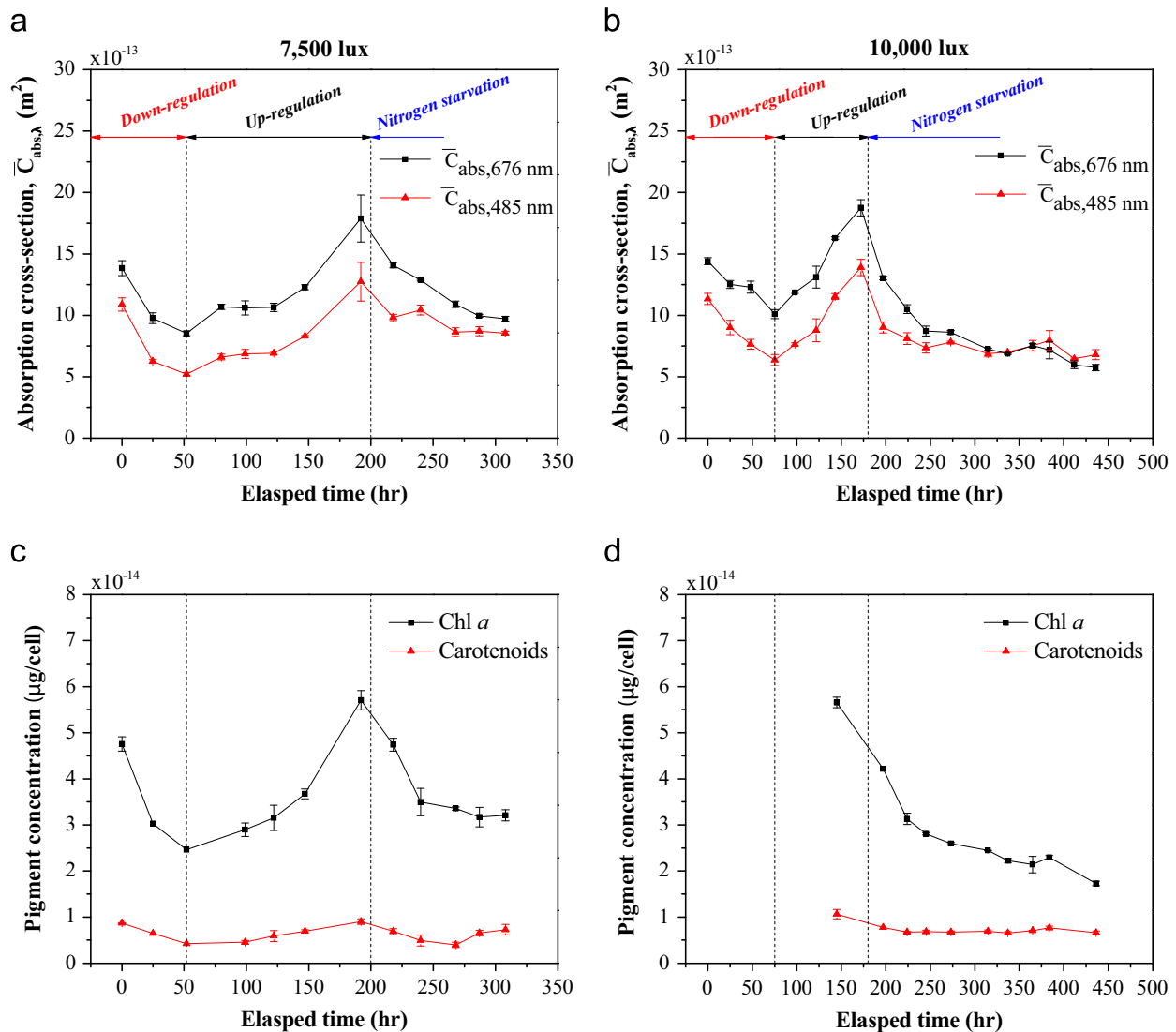


Fig. 4. (a) and (b) Temporal evolutions of average absorption cross-section at 485 and 676 nm and (c) and (d) pigment concentrations (Chl *a* and carotenoids) for *N. oculata* grown under 7500 and 10,000 lux, respectively.

in the exponential growth phase, the local fluence rate in the PBR decreased. To compensate, the microalgae synthesized additional photosynthetic pigments in order to absorb more light.

Finally, nitrogen starvation causes reduction in pigment synthesis rates [40]. As predicted from elemental analysis [27], the cultures grown under 7500 and 10,000 lux became nitrogen limited after about 200 and 180 h, respectively (Fig. 2). Interestingly, Fig. 4c and d shows that pigment concentrations decreased sharply around the same times. In fact, the culture's color changed from green to brown during nitrogen starvation due to the increase in the ratio of carotenoids to Chl *a*.

3.3. Average fluence rate and radiant power absorbed

As previously mentioned, past studies typically measured the radiation characteristics only once during the microorganisms' exponential growth phase [13–15,17,24]. Similarly, simulations of coupled light transfer and growth kinetics typically assume that radiation characteristics remain constant throughout the microalgae growth [18,21,23]. However, the spectral absorption cross-section $\bar{C}_{abs,\lambda}$ of *N. oculata* varied significantly during batch growth and reached (i) its minimum at the beginning of the exponential phase and (ii) its maximum immediately before nitrogen starvation. Here, the two-flux approximation given by Eq. (4) was used to evaluate the temporal evolution of the average fluence rate G_{ave} and the average radiant power absorbed per cell A_{ave} given by Eqs. (4) and (8), respectively. The incident radiation $G_{in,\lambda}$ was normal to the front surface of the PBR ($\theta_c = 0^\circ$) and the back surface was treated as transparent ($\rho_\lambda = 0$).

Fig. 5a and b show the evolution of the average fluence rate G_{ave} with respect to time for the cultures grown under 7500 and 10,000 lux, respectively. It was predicted using Eqs. (4)–(7) along with (i) the measured time-dependent cross-sections $\bar{C}_{abs,\lambda}$ and $\bar{C}_{sca,\lambda}$ (Fig. 3) and (ii) the values of $\bar{C}_{abs,\lambda}$ and $\bar{C}_{sca,\lambda}$ measured after about 140 h during the exponential growth phase. Predictions of G_{ave} using the measured time-dependent cross-sections $\bar{C}_{abs,\lambda}$ and $\bar{C}_{sca,\lambda}$ represent the most accurate estimate of the average fluence rate. During the lag phase or the pigment down-regulation period, G_{ave} was almost equal to G_{in} due to very low microalgae concentrations in both cultures. During the exponential growth phase, G_{ave} rapidly decreased as the microalgae simultaneously increased their number density N_T and up-regulated their pigments. Upon nitrogen starvation, G_{ave} started increasing due to the sharp decrease in pigment concentrations even though the microalgae cells continued growing. Here, G_{ave} predicted using $\bar{C}_{abs,\lambda}$ and $\bar{C}_{sca,\lambda}$ measured after ~ 140 h was adequate if the microorganisms were not in the nitrogen starvation phase when pigment concentrations decreased sharply. During the pigment down-regulation and up-regulation phases, the relative difference in G_{ave} predicted using $\bar{C}_{abs/sca,\lambda}(t)$ and $\bar{C}_{abs/sca,\lambda}(\sim 140 \text{ h})$ was less than 2% and 8% for incident irradiances of 7500 and 10,000 lux, respectively. However, it reached 45% and 57% in the nitrogen starvation phase. Therefore, in the latter phase, radiation characteristics should be measured as a function of time to predict the rapid increase in fluence rate.

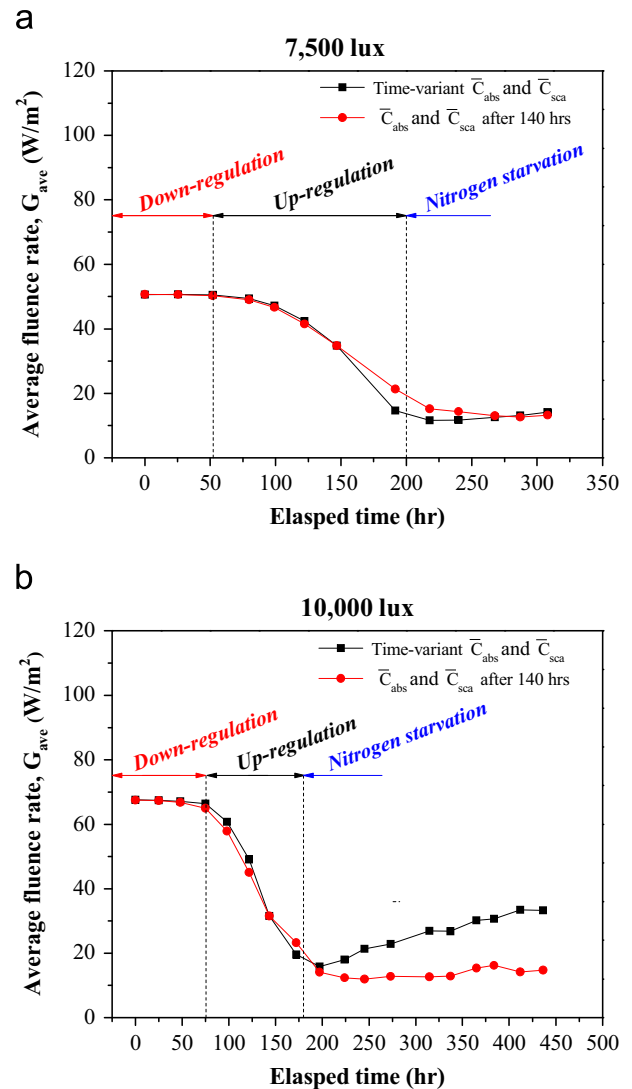


Fig. 5. Evolution of the average fluence rate in the flat-plate PBR as a function of time for cultures grown under (a) 7500 lux and (b) 10,000 lux predicted using Eqs. (4)–(7) and (i) time-dependent $\bar{C}_{abs,\lambda}$ and $\bar{C}_{sca,\lambda}$ and (ii) $\bar{C}_{abs,\lambda}$ and $\bar{C}_{sca,\lambda}$ measured after ~ 140 h during the exponential phase.

Fig. 6 shows the temporal evolution of the average radiant power absorbed per microalgae cell A_{ave} for cultures grown under 7500 and 10,000 lux predicted using Eq. (8). For both incident irradiances of 7500 and 10,000 lux, A_{ave} decreased rapidly during the down-regulation phase. This was due to the sharp decrease in pigment concentrations in response to excessive average fluence rate in the PBR. More interestingly, in the up-regulation phase, A_{ave} featured an initial increase followed by a subsequent decrease for both incident irradiances. This can be attributed to the fact that the increase in pigment concentrations (Fig. 4c and d) initially compensated for the decrease in fluence rate. However, it could not compensate for the rapid cell growth that further decreased the fluence rate and for the pigment dilution through cell division, as previously mentioned.

4. Conclusions

This paper presented the temporal evolution of the average scattering and absorbing cross-sections from 400

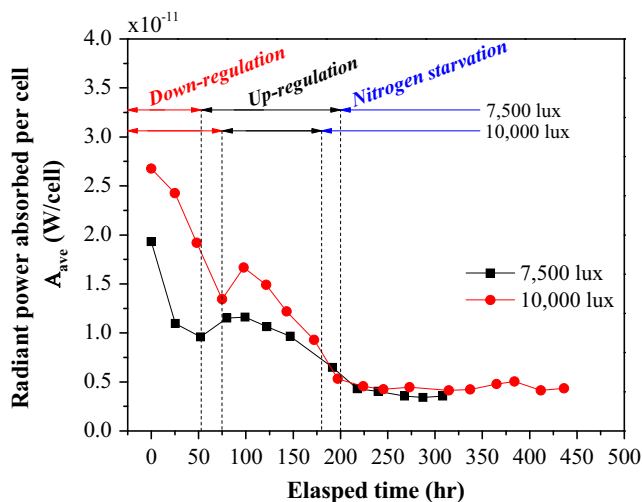


Fig. 6. Evolution of the average radiant power absorbed per microalgae cell A_{ave} [Eq. (8)] for cultures grown under 7500 and 10,000 lux.

to 750 nm for *N. oculata* grown in batch cultures under 7500 and 10,000 lux of red light at 630 nm. These cross-sections were found to vary significantly with time in response to changes in fluence rate and nutrients availability. Their evolution was interpreted in terms of up- and down-regulation of pigments and cell components in response to changing growth conditions. The observed changes in the absorption and scattering cross-sections in response to the growth conditions are likely to be representative of most microalgae by virtue of the fact that most species have similar pigments (e.g., Chl *a*) and are able to photoacclimate [9,10]. In addition, the impact on the average radiant power absorbed per cells and on the average fluence rate in the PBR was discussed. The average fluence rate in the PBR can be predicted reasonably well using radiation characteristics measured during the exponential growth phase provided that the microalgae are not nitrogen limited. In the case of nitrogen limitations, the radiation characteristics have to be measured as a function of time.

References

- [1] Richmond A. Handbook of microalgal culture: biotechnology and applied phycology. Oxford, UK: Blackwell Science Ltd; 2004.
- [2] Chisti Y. Biodiesel from microalgae. *Biotechnol Adv* 2007;25(3): 294–306.
- [3] Das D, Veziroglu TN. Hydrogen production by biological processes: a survey of literature. *Int J Hydrog Energy* 2001;26(1):13–28.
- [4] Benemann JR. Production of nitrogen fertilizer with nitrogen-fixing blue-green algae. *Enzym Microb Technol* 1979;1(2):83–90.
- [5] Barsanti L, Gualtieri P. Algae: anatomy, biochemistry, and biotechnology. Boca Raton, FL: CRC Press; 2005.
- [6] Griffiths MJ, Harrison ST. Lipid productivity as a key characteristic for choosing algal species for biodiesel production. *J Appl Phycol* 2009;21(5):493–507.
- [7] Pilon L, Berberoğlu H, Kandilian R. Radiation transfer in photobiological carbon dioxide fixation and fuel production by microalgae. *J Quant Spectrosc Radiat Transf* 2011;112(17):2639–60.
- [8] Blankenship RE. Molecular mechanisms of photosynthesis. Hoboken, NJ: Wiley-Blackwell; 2008.
- [9] Falkowski PG, LaRoche J. Acclimation to spectral irradiance in algae. *J Phycol* 1991;27(1):8–14.
- [10] Dubinsky Z, Stambler N. Photoacclimation processes in phytoplankton: mechanisms, consequences, and applications. *Aquat Microb Ecol* 2009;56:163–76.
- [11] Bidigare RR, Ondrusek ME, Morrow JH, Kiefer DA. In vivo absorption properties of algal pigments. In: Proceedings of the society of photo-optical instrumentation, Ocean Optics X, vol. 1302; 1990. p. 290–301.
- [12] Jonasz M, Fournier G. Light scattering by particles in water: theoretical and experimental foundations. San Diego, CA: Academic Press; 2007.
- [13] Berberoğlu H, Pilon L. Experimental measurement of the radiation characteristics of *Anabaena variabilis* ATCC 29413-U and *Rhodospira rubra* ATCC 49419. *Int J Hydrog Energy* 2007;32(18):4772–85.
- [14] Berberoğlu H, Pilon L, Melis A. Radiation characteristics of *Chlamydomonas reinhardtii* CC125 and its truncated chlorophyll antenna transformants *tla1*, *tlaX* and *tla1-CW+*. *Int J Hydrog Energy* 2008;33(22):6467–83.
- [15] Berberoğlu H, Gomez PS, Pilon L. Radiation characteristics of *Botryococcus braunii*, *Chlorococcum littorale*, and *Chlorella* sp. used for fixation and biofuel production. *J Quant Spectrosc Radiat Transf* 2009;110(17):1879–93.
- [16] Quirantes A, Bernard S. Light scattering by marine algae: two-layer spherical and nonspherical models. *J Quant Spectrosc Radiat Transf* 2004;89(1):311–21.
- [17] Stramski D, Mobley CD. Effects of microbial particles on oceanic optics: a database of single-particle optical properties. *Limnol Oceanogr* 1997;42(3):538–49.
- [18] Pottier L, Pruvost J, Deremetz J, Cornet J-F, Legrand J, Dussap C-G. A fully predictive model for one-dimensional light attenuation by *Chlamydomonas reinhardtii* in a torus photobioreactor. *Biotechnol Bioeng* 2005;91(5):569–82.
- [19] Dauchet J. Analyse Radiative des Photobioréacteurs [Ph.D. thesis]. France: Université Blaise Pascal, Clermont Ferrand II; 2012.
- [20] Lee E, Pilon L. Absorption and scattering by long and randomly oriented linear chains of spheres. *J Opt Soc Am A* 2013;30(9): 1892–900.
- [21] Cornet J-F, Dussap C-G, Dubertret G. A structured model for simulation of cultures of the cyanobacterium *Spirulina platensis* in photobioreactors: I. Coupling between light transfer and growth kinetics. *Biotechnol Bioeng* 1992;40(7):817–25.
- [22] Cornet J-F, Dussap C-G. A simple and reliable formula for assessment of maximum volumetric productivities in photobioreactors. *Biotechnol Progr* 2009;25(2):424–35.
- [23] Slegers PM, Wijffels RH, Van Straten G, Van Boxtel AJB. Design scenarios for flat panel photobioreactors. *Appl Energy* 2011;88(10): 3342–53.
- [24] Morel A, Bricaud A. Inherent optical properties of algal cells including picoplankton: theoretical and experimental results. *Can Bull Fish Aquat Sci* 1986;214:521–59.
- [25] Rodolfi L, Chini Zittelli G, Bassi N, Padovani G, Biondi N, Bonini G, et al. Microalgae for oil: strain selection, induction of lipid synthesis and outdoor mass cultivation in a low-cost photobioreactor. *Biotechnol Bioeng* 2009;102(1):100–12.
- [26] Ke B. Photosynthesis photobiology and photobiophysics. Dordrecht, The Netherlands: Kluwer Academic Publishers; 2001.
- [27] Kandilian R, Lee E, Pilon L. Radiation and optical properties of *Nannochloropsis oculata* grown under different irradiances and spectra. *Bioresour Technol* 2013;137:63–73.
- [28] Modest M. Radiative heat transfer. 2nd ed San Diego, CA: Academic Press; 2003.
- [29] Davies-Colley RJ, Pridmore RD, Hewitt JE. Optical properties of some freshwater phytoplanktonic algae. *Hydrobiologia* 1986;133(2): 165–78.
- [30] Agrawal BM, Mengüç MP. Forward and inverse analysis of single and multiple scattering of collimated radiation in an axisymmetric system. *Int J Heat Mass Transf* 1991;34(3):633–47.
- [31] Privoznik KG, Daniel KJ, Incropera FP. Absorption, extinction and phase function measurements for algal suspensions of *Chlorella pyrenoidosa*. *J Quant Spectrosc Radiat Transf* 1978;20(4):345–52.
- [32] van de Hulst HC. Light scattering by small particles. Mineola, NY: Courier Dover Publications; 2012.
- [33] Wellburn AR. The spectral determination of chlorophylls *a* and *b*, as well as total carotenoids, using various solvents with spectrophotometers of different resolution. *J Plant Physiol* 1994;144(3):307–13.
- [34] Strickland JD, Parsons TR. A practical handbook of seawater analysis. Ottawa, Canada: Fisheries Research Board of Canada; 1968.
- [35] Becker EW. Microalgae: biotechnology and microbiology, vol. 10. Cambridge, UK: Cambridge University Press; 1994.
- [36] Chiu S-Y, Kao C-Y, Tsai M-T, Ong S-C, Chen C-H, Lin C-S. Lipid accumulation and CO₂ utilization of *Nannochloropsis oculata* in response to CO₂ aeration. *Bioresour Technol* 2009;100(2):833–8.
- [37] Simionato D, Sforza E, Corteggiani Carpinelli E, Bertuccio A, Giacometti GM, Morosinotto T. Acclimation of *Nannochloropsis gaditana* to

- different illumination regimes: effects on lipids accumulation. *Bioresour Technol* 2011;102(10):6026–32.
- [38] Aas E. Refractive index of phytoplankton derived from its metabolite composition. *J Plankton Res* 1996;18(12):2223–49.
- [39] Renaud SM, Parry DL, Thinh L-V, Kuo C, Padovan A, Sammy N. Effect of light intensity on the proximate biochemical and fatty acid composition of *Isochrysis* sp. and *Nannochloropsis oculata* for use in tropical aquaculture. *J Appl Phycol* 1991;3(1):43–53.
- [40] de Vasconcelos L, Fay P. Nitrogen metabolism and ultrastructure in *Anabaena cylindrica*. *Arch Microbiol* 1974;96(1):271–9.